JOURNAL OF VIROLOGY, June 2004, p. 6360–6369 Vol. 78, No. 12
0022-538X/04/$08.00+0 DOI: 10.1128/JVI.78.12.6360–6369.2004


# Novel Nuclear Herniations Induced by Nuclear Localization of a Viral Protein

Cristen C. Hoyt,[1] Ron J. Bouchard,[2] and Kenneth L. Tyler[1,2,3,4,5,6]*

*Departments of Immunology,[1] Microbiology,[6] Neurology,[3] and Medicine[4] and Program in Neurosciences,[5] University of Colorado Health Sciences Center, and Denver Veterans Affairs Medical Center,[2] Denver, Colorado 80262*

Received 15 December 2003/Accepted 5 February 2004

**A common consequence of viral infection is perturbation of host cell nuclear functions. For cytoplasmically replicating viruses, this process may require regulated transport of specific viral proteins into the nucleus. Here, we describe a novel form of virus-induced perturbation of host cell nuclear structures. Active signal-mediated nuclear import of the reovirus σ1s protein results in redistribution of nuclear pore complexes and nuclear lamins and formation of nuclear herniations. These herniations represent a previously undescribed mechanism by which cytoplasmic viral infection can perturb nuclear architecture and induce cytopathic effects, which ultimately lead to disease pathogenesis in the infected host.**

Mammalian reoviruses provide an important experimental model for understanding viral pathogenesis and virus-host interactions at a cellular level (40). Although reovirus replication occurs in the cytoplasm, infection disrupts a variety of host cell nuclear functions, resulting in a virus-induced cytopathic effect in infected cells and tissue injury in the infected host. For example, reovirus infection results in activation of specific cellular signaling pathways and their associated transcription factors (4–6), alteration of host cell gene expression (9, 30), perturbation of cell cycle regulation (31, 32), and induction of apoptosis (40, 41).

The mechanisms responsible for reovirus-induced alteration of nuclear function and the viral genes and proteins involved are only beginning to be characterized. For example, reovirus-induced inhibition of host cellular proliferation results from a cell cycle arrest at the $G_2$/M checkpoint (32). Studies using a mutant reovirus and protein expression studies indicate that σ1s, a nonstructural protein encoded by the reovirus S1 gene, is necessary and sufficient for reovirus-induced $G_2$/M cell cycle arrest (32). σ1s-mediated changes in cell cycle regulation are associated with changes in the activities and phosphorylation states of key $G_2$/M-regulatory kinases, including p34 (cdc2) (31).

Like reoviruses, many other viruses perturb cell cycle regulation and other host cell nuclear functions, presumably in order to promote an optimal environment for viral replication. These viral effects on host cell nuclear functions can be mediated through a variety of mechanisms, including alteration of nuclear architecture (17, 18, 26, 37), disruption of nucleocytoplasmic transport pathways (12, 14, 27, 28), and induction of nuclear herniations (10). For cytoplasmically replicating viruses, the nuclear envelope (NE) acts as a protective boundary preventing indiscriminate interaction between cytoplasmic viral proteins and the nucleus. The NE consists of the outer and inner nuclear membranes, nuclear pore complexes (NPCs), and the underlying nuclear lamina. The nuclear lamina organizes the distribution of NPCs (20), provides shape to the nucleus (39), and plays a role in chromatin organization (16). Embedded within the NE are large multiprotein NPC structures that regulate bidirectional macromolecular traffic between the nucleus and cytoplasm in eukaryotic cells. One mechanism by which viral proteins can traverse the NE is through active nucleocytoplasmic transport. This process can be mediated by the binding of cellular nuclear transport receptors (importins) to specific nuclear localization signals (NLS) in viral proteins. The viral protein complex docks at the cytoplasmic face of the NPC, following which the viral cargo is imported through the NPC and into the nucleus. Once inside the nucleus, viral proteins can interact with specific nuclear structures (15, 28, 44), nuclear proteins (19, 45), or chromatin (22, 35) to alter nuclear function.

Early immunocytochemical studies suggested that σ1s could be detected in the nucleus during reovirus infection (1, 34); however, definitive evidence of σ1s nuclear localization, the mechanism by which this occurs, and its potential effects on nuclear function have been lacking. We now show that reovirus σ1s is actively localized to the nucleus, utilizing a previously unrecognized NLS. Nuclear localization of σ1s induces profound structural defects in chromatin, disrupts nuclear lamina, and induces clustering of NPCs and the formation of nuclear herniations. These effects represent a novel type of virus-induced damage to host cell nuclear architecture, which provides a previously undescribed mechanism by which a cytoplasmically replicating virus can perturb nuclear function.

## MATERIALS AND METHODS

**Cells and viruses.** Mouse L929 cells were grown in minimal essential medium (Gibco/Invitrogen, Carlsbad, Calif.) supplemented to contain 5% heat-inactivated fetal bovine serum (Gibco/Invitrogen), 1 mM nonessential amino acids (Gibco/Invitrogen), and 2 mM L-glutamine (Gibco/Invitrogen). Human HeLa cells were grown in minimal essential medium (Gibco/Invitrogen) supplemented to contain 10% fetal bovine serum (Gibco/Invitrogen), 1 mM nonessential amino acids (Gibco/Invitrogen), and 2 mM L-glutamine (Gibco/Invitrogen). Cell monolayers were grown on eight-well glass chamber slides. Type 3 Abney (T3A)

* Corresponding author. Mailing address: Department of Neurology (B-182), University of Colorado Health Sciences Center, 4200 E. 9th Ave., Denver, CO 80262. Phone: (303) 393-2874. Fax: (303) 393-4686. E-mail: Ken.Tyler@uchsc.edu.

reovirus was used as wild-type reovirus and is a laboratory stock. Type 3 reovirus clone 84-MA (T3C84-MA) was used as σ1s null mutant reovirus and was originally isolated via serial passage of T3C84 through murine erythroleukemia cells (34).

**Plasmids.** A cDNA of reovirus T3A σ1s was generated by reverse transcriptase PCR amplification from purified T3A double-stranded RNA by using primers specific for the σ1s ORF. Chicken pyruvate kinase fused to green fluorescent protein (pEGFP-PK) was a generous gift (38). T3A σ1s cDNA was cloned between green fluorescent protein (GFP) and chicken pyruvate kinase by using HindIII and BglII restriction sites to generate the GFP-σ1s-PK vector. Mutation constructs GFP-No NLS σ1s-PK and σ1s NLS-GFP-PK were derived from GFP-σ1s-PK by introducing specific amino acid changes via site-directed mutagenesis.

**Transfection.** L929 and HeLa cells were grown on glass chamber slides to 80% confluency. L929 cell DNA transfections were carried out with the Lipofectamine 2000 reagent by a method based on the recommended protocol described by the manufacturer (Gibco/Invitrogen). HeLa cell DNA transfections were carried out with the CalPhos mammalian transfection kit (BD Biosciences Clontech, Palo Alto, Calif.) by a method based on the recommended protocol described by the manufacturer.

**Immunocytochemistry.** Posttransfection, cells were washed in phosphate-buffered saline and fixed in fresh 3.7% paraformaldehyde in phosphate-buffered saline for 15 min (Fischer). Nuclei were visualized with Hoechst 33342 double-stranded DNA (dsDNA) stain (Molecular Probes, Eugene, Oreg.). GFP fusion proteins were visualized directly by digital fluorescence microscopy. For indirect immunofluorescence analysis, L929 or HeLa cells plated on glass chamber slides were fixed in 3.7% paraformaldehyde for 15 min, permeabilized with 0.1% Triton X-100–3 to 5% bovine serum albumin overnight at 4°C, blocked in 3 to 5% bovine serum albumin at 25°C for 1 h, and incubated with primary antibody overnight at 4°C. The antibodies used were as follows: mouse monoclonal anti-C23 antibody (1:100; Santa Cruz Biotechnology, Santa Cruz, Calif.), mouse monoclonal anti-nuclear transport factor p97/importin β antibody (1:1,000; Affinity BioReagents, Golden, Colo.), mAb414 (antinucleoporin antibody) (1:1,000; Covance/BabCo, Richmond, Calif.), and mouse monoclonal anti-lamin A and C (anti-LaA/C) (1:500; Covance/BabCo). The hybridoma cell line synthesizing the anti-σ1s antibody, 2F4, was a generous gift (34). Anti-σ1s was purified on a protein A column by a method based on the recommended protocol described by the manufacturer (Pierce, Rockford, Ill.). After being washed, cells were incubated with secondary horse anti-mouse immunoglobulin G conjugated to Texas red (1:100; Vector Laboratories, Inc., Burlingame, Calif.) for 1 h at 25°C. Cells were washed, and nuclei were visualized with Hoechst 33342 dsDNA stain and examined via deconvolution microscopy. Cellular expression patterns were quantified by examining approximately 100 cells/field. Three independent cell counts from different fields were normalized for graphing and statistically analyzed with In Stat version 3.0 (GraphPad, San Diego, Calif.).

**Microscopy.** Cells for transmission electron microscopy were fixed in 2.5% glutaraldehyde, postfixed in 2% osmium tetroxide, dehydrated in a graded series of alcohol solutions, and embedded in epoxy resin. Sections, approximately 80 nm in thickness, were stained with uranyl acetate and lead citrate prior to examination at 60 kV with a transmission electron microscope (Zeiss EM-10). Cells for digital fluorescence microscopy were imaged under oil immersion with a 63× Plan-Apochromate objective (Zeiss Axioplan 2 digital microscope with Cooke sensiCam 12-bit camera). Cells for digital deconvolution microscopy were imaged under oil immersion with a 63× Plan-Apochromate objective, and by using nearest neighbor (Slidebook software; Intelligent Imaging Innovations, Denver, Colo.), multiple 0.5-μm planes were deconvolved into an image in which blur and artifact had been digitally removed. Three-view images (*x* and *y* cross-sections) are expansions of deconvolved images in which orthogonal planes can be seen simultaneously.

**Nucleotide sequence accession numbers.** The NCBI accession number for T3A ($\sigma1s^+$ reovirus) is L37677, and the NCBI accession number for T3 C84-MA ($\sigma1s^-$ reovirus) is U74291.

## RESULTS

**σ1s localization during reovirus infection.** The subcellular localization of T3A σ1s was determined by immunocytochemistry and deconvolution microscopy with the σ1s-specific monoclonal antibody 2F4. Deconvolution of multiple planes through *x*, *y*, and *z* axes of reovirus-infected L929 cells (Fig. 1A to C) and reovirus-infected HeLa cells (Fig. 1D to F) at 24 h postinfection clearly demonstrates the presence of σ1s in the cytoplasm and within nuclear boundaries as evidenced by the *x* and *y* plane cross-section images (Fig. 1A and D). σ1s occupies discrete nuclear subareas as evidenced by the appearance of separate zones of σ1s interlaced with distinct areas of chromatin in the *x* and *y* cross-sections (Fig. 1A and D). In infected L929 cells the distributions of σ1s in the nucleus and cytoplasm are approximately equivalent (Fig. 1B). However, in HeLa cells σ1s appears to preferentially localize to the nucleus (Fig. 1E). The σ1s localization patterns shown persist through 48 h postinfection.

**Active signal-mediated nuclear import of σ1s.** We expressed the 14-kDa σ1s protein as a fusion with the cytoplasmic reporter protein, GFP-PK (38) (GFP-σ1s-PK) (Fig. 2E). The large size of the GFP-σ1s-PK fusion protein ensured that nuclear localization was dependent upon active σ1s signal-mediated nuclear import and was not a result of passive diffusion. L929 cells were transiently transfected with either GFP-PK (Fig. 2B to D) or GFP-σ1s-PK (Fig. 2F to H) and analyzed at 24 h posttransfection via digital fluorescence microscopy. Constructs lacking σ1s were restricted to the cytoplasm (Fig. 2B). Insertion of σ1s resulted in significant redistribution of GFP-PK to the nucleus (Fig. 2F). σ1s also imparted nuclear localization to GFP-PK in HeLa cells (data not shown). The percentage of cells exhibiting nuclear localization of the reporter construct compared to exclusively cytoplasmic localization is shown in Fig. 2I.

Examination of the σ1s nuclear localization pattern in both reovirus-infected and σ1s-transfected cells suggested that the protein was not uniformly distributed throughout the nucleus (Fig. 2H). We used an antibody against nucleolin to define nucleolar boundaries during GFP-σ1s-PK transfection of L929 cells. The nuclear expression pattern of GFP-σ1s-PK was distinctly segregated from nucleolar regions (Fig. 2J to L). Using deconvolution microscopy to image multiple sections through L929 cells expressing GFP-σ1s-PK in the *x*, *y*, and *z* planes, we found that GFP-σ1s-PK was located both in the cytoplasm and within nuclear boundaries but was excluded from nucleolar regions of cell nuclei (Fig. 2 M, top and side panels). These studies indicate that both transfected σ1s and virion-encoded σ1s synthesized in cells during natural infection can translocate to the nucleus and that the σ1s protein contains an NLS that can mediate nuclear localization of a cytoplasmic reporter protein.

**A novel σ1s NLS.** Sequence analysis of σ1s suggested the presence of a putative σ1s NLS, $^{15}$RSRRRLK$^{21}$, within a conserved arginine-rich region (11) near the N terminus of the protein. In order to ascertain whether this putative σ1s NLS was functional, site-directed mutagenesis was performed to remove residues $^{15}$RSRRRLK$^{21}$ from σ1s in the context of the GFP-σ1s-PK construct (Fig. 3C, schematic) (GFP-No NLS σ1s-PK). L929 cells were transiently transfected with GFP-PK (Fig. 3A), GFP-σ1s-PK (Fig. 3B), or GFP-No NLS σ1s-PK (Fig. 3C) and analyzed at 24 posttransfection via digital florescence microscopy. Removal of the putative σ1s NLS significantly disrupted σ1s-mediated nuclear localization of GFP-σ1s-PK (Fig. 3C and E). Similar results were found for GFP-σ1s-PK-transfected HeLa cells (data not shown). σ1s amino acids $^{15}$RSRRRLK$^{21}$ were then added to the cytoplasmic GFP-PK protein to determine whether the σ1s NLS alone was sufficient to mediate nuclear localization of the reporter protein (Fig. 3D) (σ1s NLS-GFP-PK). Transfection of L929 cells with σ1s NLS-GFP-PK resulted in significant nuclear localiza-

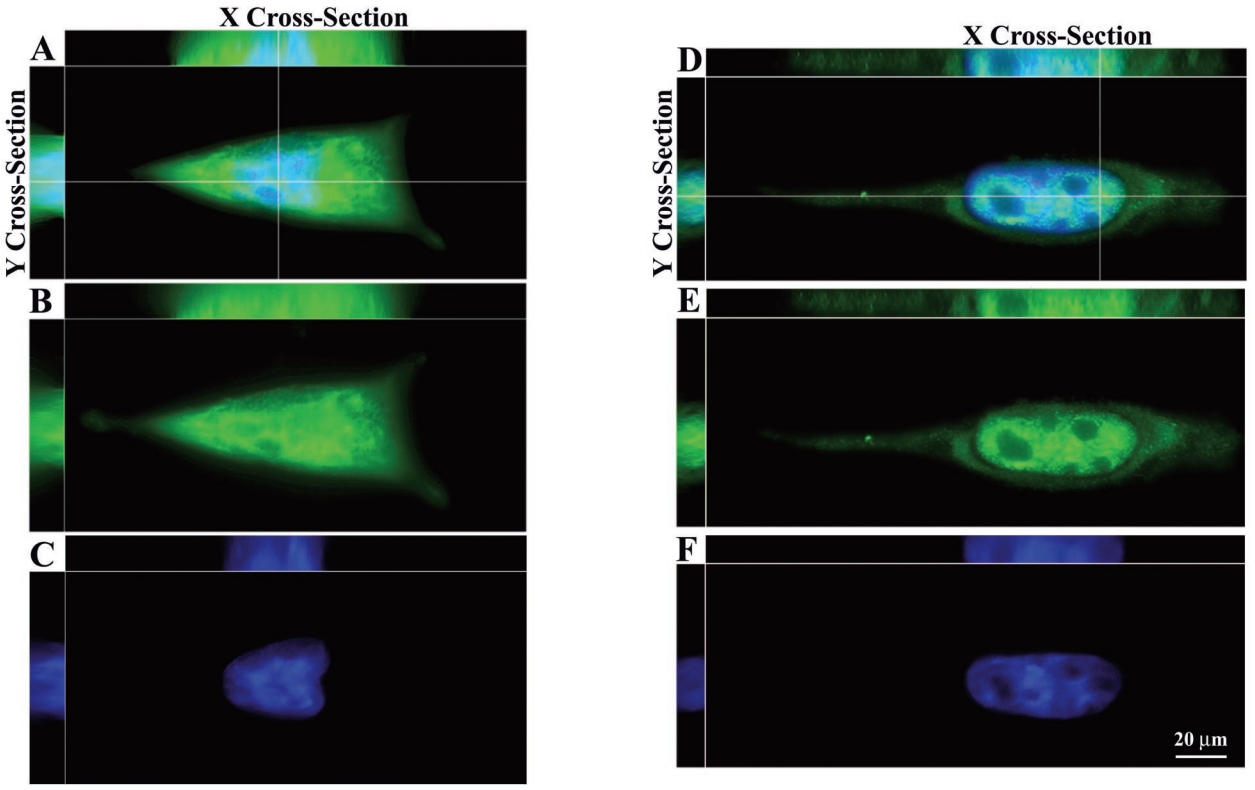


FIG. 1. σ1s localizes to the nucleus and cytoplasm during natural virus infection. L929 cells (A to C) and HeLa cells (D to F) were infected with reovirus for 24 h and stained with a monoclonal antibody directed against σ1s. (B and E) Monoclonal antibody staining was followed by a fluorescein isothiocyanate-conjugated secondary antibody. (C and F) Hoechst 33342 dsDNA stain was used to define the misshapen nuclei of σ1s-expressing cells. (A and D) Deconvolution microscopy was used to analyze σ1s subcellular and subnuclear localization in multiple *x*, *y*, and *z* planes in the merged images. σ1s localizes to the nucleus in infected cells but does not colocalize with chromatin (A and D).

tion of GFP-PK compared to cells transfected with reporter protein alone (Fig. 3F). These results indicate that σ1s residues $^{15}$RSRRRLK$^{21}$ comprise a novel σ1s NLS which is both necessary and sufficient for nuclear localization.

**σ1s-induced nuclear herniations and infection.** In our studies of σ1s localization we observed that infection of cells with wild-type reovirus was associated with dramatic alterations in the shape and distribution of nuclear chromatin (Fig. 1C and F). In order to determine whether σ1s was required for these effects, we tested a σ1s null mutant reovirus (σ1s$^-$ virus) for the presence of similar chromatin abnormalities during viral infection. The σ1s null mutant reovirus is unable to express σ1s due to a mutation in the S1 gene segment which introduces a premature stop codon at amino acid 6 in the σ1s sequence (34). In cell culture σ1s-deficient reovirus grows as well as its σ1s$^+$ parent virus and induces equivalent levels of apoptosis (34) but does not induce $G_2$/M cell cycle arrest due to the loss of σ1s expression (32).

Following infection of HeLa cells with wild-type reovirus (σ1s$^+$ virus), chromatin appeared to be misshapen and decompacted as indicated by heterogeneity in Hoechst 33442 staining (Fig. 4A). These changes were not seen following σ1s$^-$ virus infection, during which Hoechst 33442 staining remained homogenous and with an undistorted shape (Fig. 4D). These data suggested that the presence of σ1s in the nucleus was the cause of the observed changes in nuclear architecture and chromatin organization.

Consistent with the observed irregularities in chromatin organization, examination of σ1s$^+$ virus-infected cell nuclei by differential interference contrast (DIC) microscopy revealed structural alterations in nuclear shape, which were not seen during σ1s$^-$ virus infection (Fig. 4, B and E). In σ1s$^-$ virus-infected cells, nuclei were generally round or ovoid with smooth nuclear contours (Fig. 4E), whereas cells infected with σ1s$^+$ virus contained nuclei of irregular shape with marked nuclear herniations containing DNA (Fig. 4A and B).

Thin-section electron microscopy was used to further examine the relationship between σ1s and the nuclear morphology of reovirus-infected cells. Consistent with DIC microscopy, nuclei of σ1s$^+$ virus-infected HeLa cells were highly lobulated and misshapen, with prominent nuclear herniations evident (Fig. 5A). The cytoplasm of both σ1s$^+$ virus-infected and σ1s$^-$ virus-infected cells showed no changes other then the presence of replicating reovirus (Fig. 5). The chromatin of both σ1s$^+$ virus-infected and σ1s$^-$ virus-infected HeLa cells was surrounded by an intact NE and did not appear to be undergoing margination or compaction as is characteristic of later stages of reovirus-induced apoptosis (41).

Since disruption of the NE affects nuclear shape (20), we used an antibody against importin-β to examine the consistency of the NE framework. The nuclear import receptor importin-β defines both the contoured boundaries of the nuclear envelope and the integrity of specific nuclear import components within the NE by its ability to form an import complex

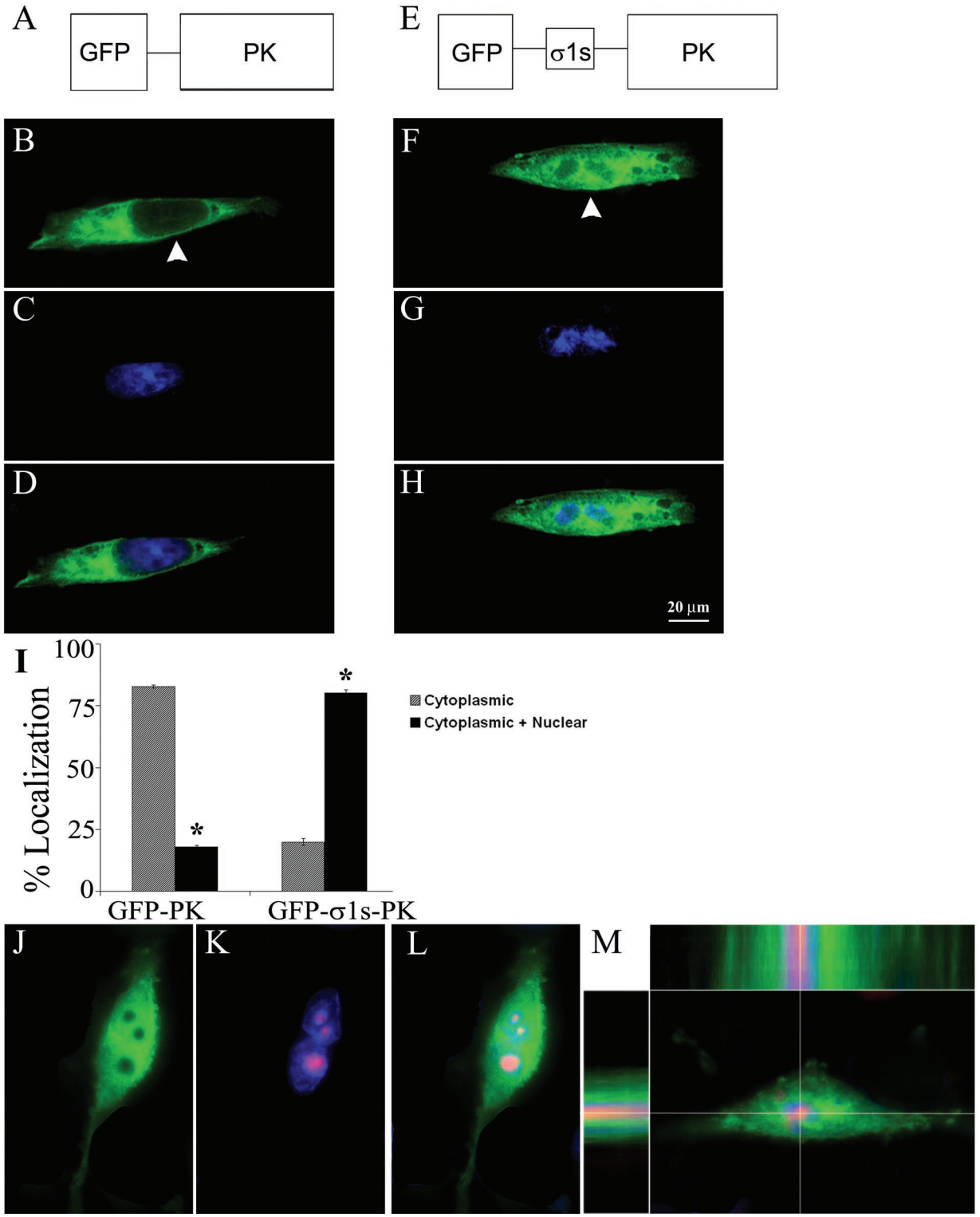


FIG. 2. σ1s imparts nuclear localization to a cytoplasmic reporter protein and does not localize to the nucleolus. (A) Schematic of GFP-PK fusion protein. (E) Schematic of GFP-σ1s-PK fusion protein. (B to D and F to H) L929 cells were transiently transfected with GFP-PK (B to D) or GFP-σ1s-PK (F to H). Hoechst 33342 dsDNA stain was used to define nuclei (C and G). Arrowheads indicate localization of fusion proteins. GFP-σ1s-PK significantly (*) ($P < 0.001$) localized to the nucleus (I) and did not colocalize with misshapen chromatin (G and H). (J to M) GFP-σ1s-PK-transfected L929 cells were stained with a monoclonal antibody directed against nucleolin followed by a Texas-red conjugated secondary antibody to demonstrate that GFP-σ1s-PK does not localize to nucleolar regions. Deconvolution microscopy was used to analyze subcellular and subnuclear localization in multiple *x*, *y*, and *z* planes (top and side bars in panel M).

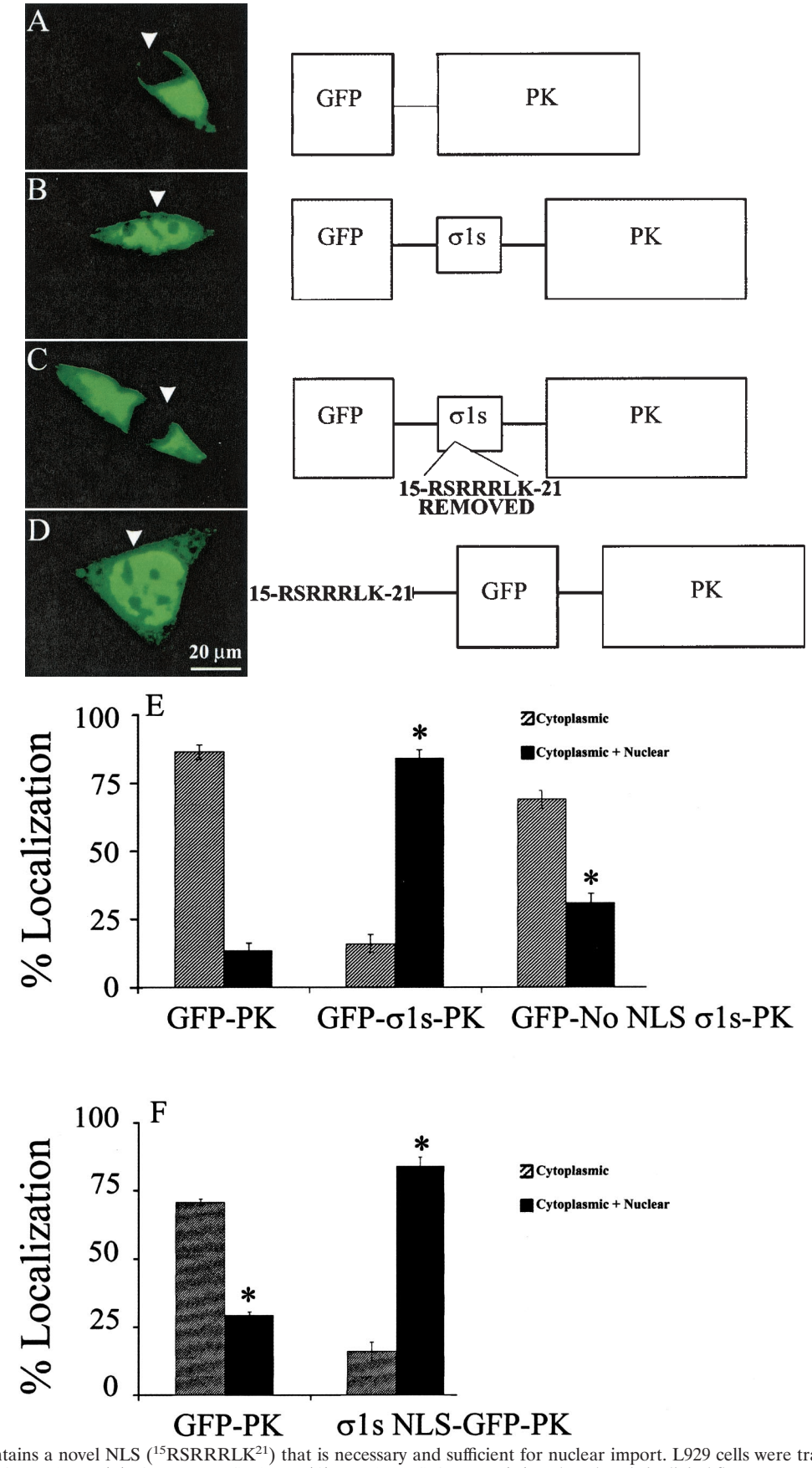


FIG. 3. σ1s contains a novel NLS ($^{15}$RSRRRLK$^{21}$) that is necessary and sufficient for nuclear import. L929 cells were transiently transfected with GFP-PK (A), GFP-σ1s-PK (B), GFP-No NLS σ1s-PK (C), or σ1s NLS-GFP-PK (D) and analyzed via digital florescence microscopy. Removal of the σ1s NLS from GFP-σ1s-PK resulted in significant (*) ($P < 0.001$) loss of nuclear localization (E) while addition of the σ1s NLS resulted in significant translocation to the nucleus (F). σ1s amino acids $^{15}$RSRRRLK$^{21}$ comprise a previously undiscovered NLS.

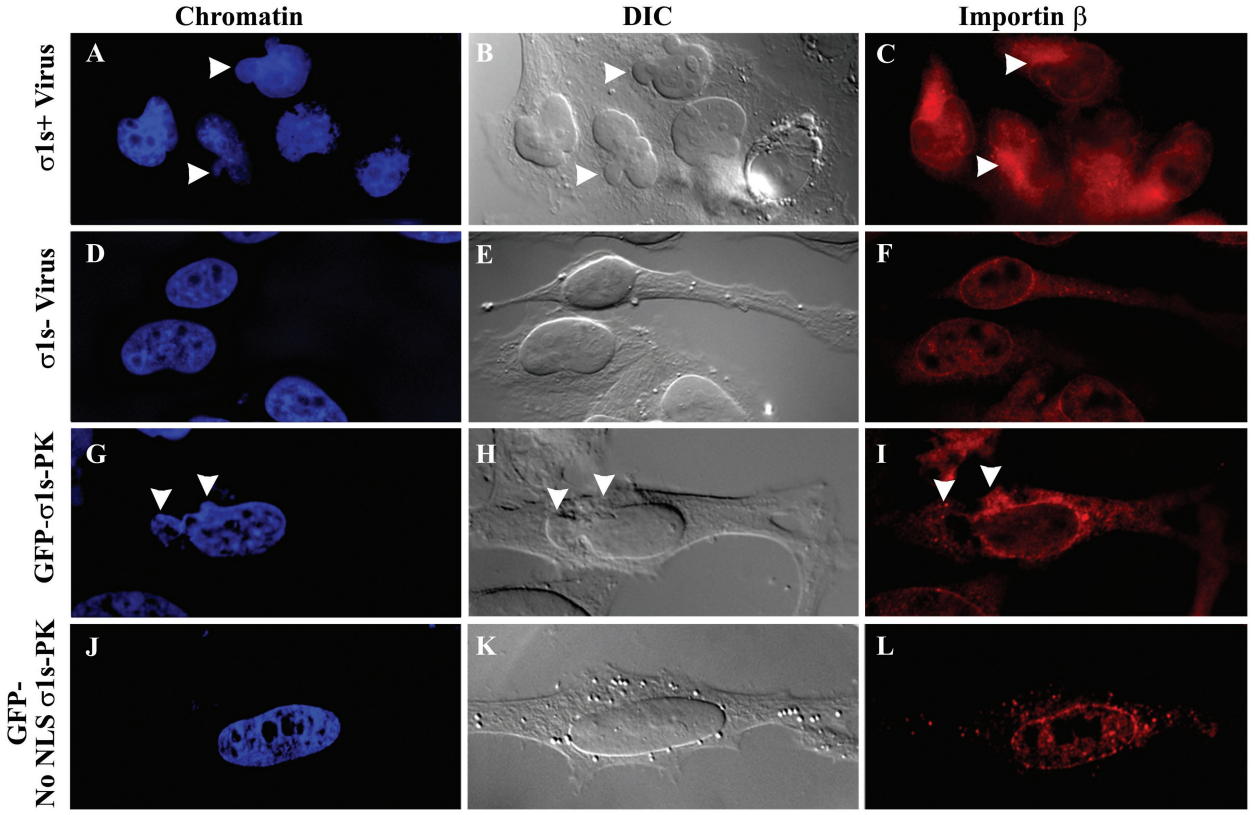


FIG. 4. σ1s nuclear localization induces nuclear herniations during natural virus infection and σ1s transfection. HeLa cells were infected with wild-type reovirus ($\sigma1s^+$ virus) (A to C) or σ1s null reovirus ($\sigma1s^-$ virus) (D to F) for 24 h. Hoechst 33342 dsDNA stain was used to define nuclei (A, D, G, and J). $\sigma1s^+$ virus-infected cells induced localized disruption in nuclear morphology (arrowheads in panel B) and chromatin staining (arrowheads in panel A) compared to cells infected with the mutant reovirus that does not produce σ1s (D and E). The nuclear envelope remained intact in $\sigma1s^+$ virus-infected cells and displayed areas of importin-β clustering, suggestive of NPC clustering (arrowheads in panel C) while $\sigma1s^-$ virus-infected cells retained typical nuclear morphology, chromatin, and importin-β staining (D to F). GFP-σ1s-PK-transfected HeLa cells displayed identical alterations in nuclear morphology, chromatin staining, and importin-β clustering (arrowheads in panels G to I) compared to cells expressing σ1s only in the cytoplasm (J to L). σ1s induces disruption in nuclear morphology (arrowheads in panel H), chromatin staining (arrowheads in panel G), and importin-β (arrowheads in panel I) only when localized in the nucleus.

containing NLS-containing protein cargo, dock the import complex at the cytoplasmic face of the NPC, and release it at the nucleoplasmic face of the NE (7). In $\sigma1s^+$ virus-infected cells, importin-β staining showed that the NE remained intact and encompassed the altered nuclear contour (Fig. 4C). Consistent with spacing of NPCs throughout the NE, importin-β staining maintained a punctate pattern throughout the NEs of $\sigma1s^-$ virus-infected cells (Fig. 4F). In contrast, in $\sigma1s^+$ virus-infected cells, importin-β staining showed a pattern of areas of dense positive staining localized to the cytoplasmic face of nuclear herniations, which is suggestive of clustered NPCs at nuclear herniation sites (Fig. 4C).

**σ1s nuclear import and nuclear herniations.** The conclusion that virally encoded σ1s expressed during infection induces nuclear herniations is further strengthened by the finding that identical alterations in NE morphology were seen when σ1s was expressed alone. As seen with viral infection, GFP-σ1s-PK transfection of L929 cells (Fig. 2G) and HeLa cells (Fig. 4G) induces chromatin abnormalities. When σ1s was inhibited from entering the nucleus due to removal of the σ1s NLS (GFP-No NLS σ1s-PK) the nucleus maintained the smooth contour and unaltered symmetric morphology of nontransfected cells and the chromatin remained of a uniform and undistorted shape (Fig. 4J and K). By contrast, nuclear expression of σ1s grossly altered the nuclear contour and chromatin staining intensity and shape (Fig. 4G and H). Despite the presence of an altered nuclear shape seen in the DIC image induced by σ1s nuclear localization (Fig. 4H), the NEs of GFP-σ1s-PK-expressing cell nuclei remained intact and encompassed the altered nuclear contour (Fig. 4I). Similarly to $\sigma1s^+$ virus-infected cells, GFP-σ1s-PK-expressing cells exhibited cytoplasmic clustering of importin-β in areas of nuclear herniations (Fig. 4I), again suggesting that although NPCs are positioned throughout the NE, they appear to be clustered within areas of nuclear herniations. In summary, both σ1s transfection and σ1s expression during natural virus infection induced nuclear herniations distinguished by misshapen chromatin, abnormal nuclear morphology, and importin-β clustering. These data indicate that σ1s is both necessary and sufficient for herniation development and that the appearance of nuclear herniations required the presence of σ1s in the nuclei of cells.

**NPC clustering and nuclear lamina disruption.** As suggested by the pattern of importin-β staining, antibodies to NPC

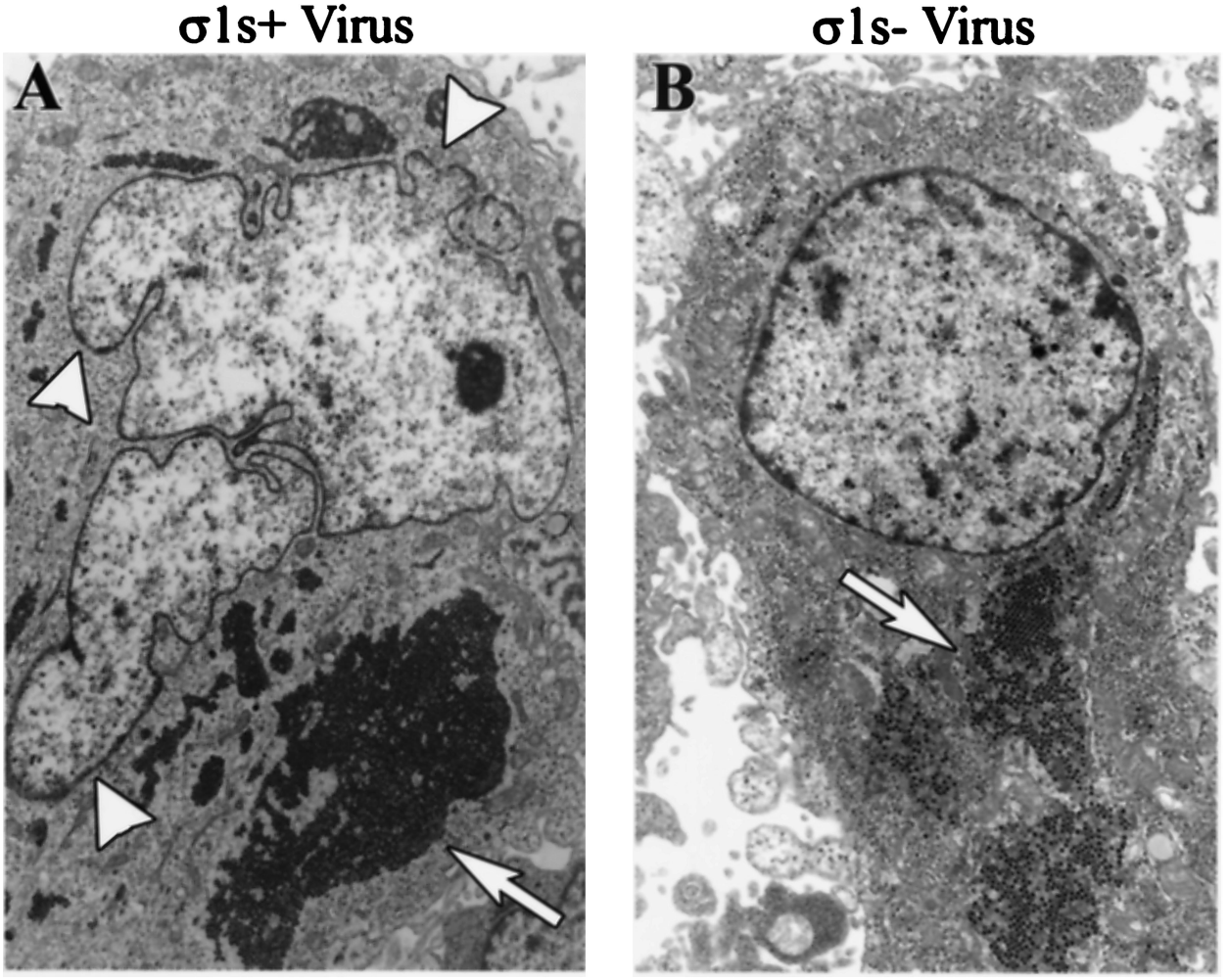


FIG. 5. σ1s induces nuclear herniations during natural virus infection. HeLa cells were infected with wild-type reovirus ($\sigma1s^+$ virus) (A) or σ1s null reovirus ($\sigma1s^-$ virus) (B) for 24 h. Thin-section electron microscopy was used to image nuclear architecture changes induced by σ1s expression. σ1s induces nuclear herniations (arrowheads in panel A). Both wild-type and σ1s null reovirus are present in the cytoplasm (arrows).

proteins (nucleoporins) confirmed clustering of NPCs in areas of σ1s-induced nuclear herniations. Nucleoporin labeling of cells lacking σ1s in the nucleus (GFP-No NLS σ1s-PK) showed uninterrupted punctate NE rim and NE surface staining characteristic of the regular distribution of NPC (2) throughout the NE (Fig. 6D to F and J to L). Conversely, cells in which σ1s was expressed in the nucleus (GFP-σ1s-PK) exhibited clustering of NPC in areas of σ1s-induced nuclear herniations seen at both the rim and the surface of the NE (Fig. 6B and H). Although some rim-like NPC staining was apparent in nuclei of these cells (Fig. 6B), the remainder of the NE was usually barren of NPC (Fig. 6B). This can be seen more directly by looking at the surface of the nucleus in which the NE was depleted of NPCs in specific areas (Fig. 6H) balanced by others areas with clustered NPCs near herniation sites (Fig. 6H), while minor regions of the NE appeared to have NPCs in a regular distribution.

An intact nuclear lamina helps govern correct spacing of NPCs and helps maintain normal nuclear shape (13, 21, 23). The type V intermediate filament proteins lamins A and C are major components of the nuclear lamina and polymerize in various ratios to form a filamentous scaffold which maintains nuclear shape and integrity (24, 39). The observed σ1s-mediated abnormalities in nuclear shape and σ1s-induced clustering of NPC and herniation development could result from perturbation of the nuclear lamina organization. A monoclonal antibody against A-type nuclear LaA/C was used to stain HeLa cells transfected with GFP-σ1s-PK (Fig. 7A to C) or GFP-No NLS σ1s-PK (Fig. 7D to F) constructs. In contrast to the round or ovoid nuclei of nontransfected cells (data not shown) or to GFP-No NLS σ1s-PK-transfected cells, which display normal continuous nuclear rim LaA/C staining (Fig. 7F), GFP-σ1s-PK-expressing cell nuclei displayed marked abnormalities in the A-type lamina network (Fig. 7C). Within the nucleus, σ1s induced highly localized defects in the nuclear lamina at sites of herniations, which appeared as LaA/C gaps (Fig. 7C). In addition, LaA/C accumulated at other points throughout the nucleus, sometimes at the base of herniations, as seen by increased intensity of LaA/C staining (Fig. 7C). Thus, both the

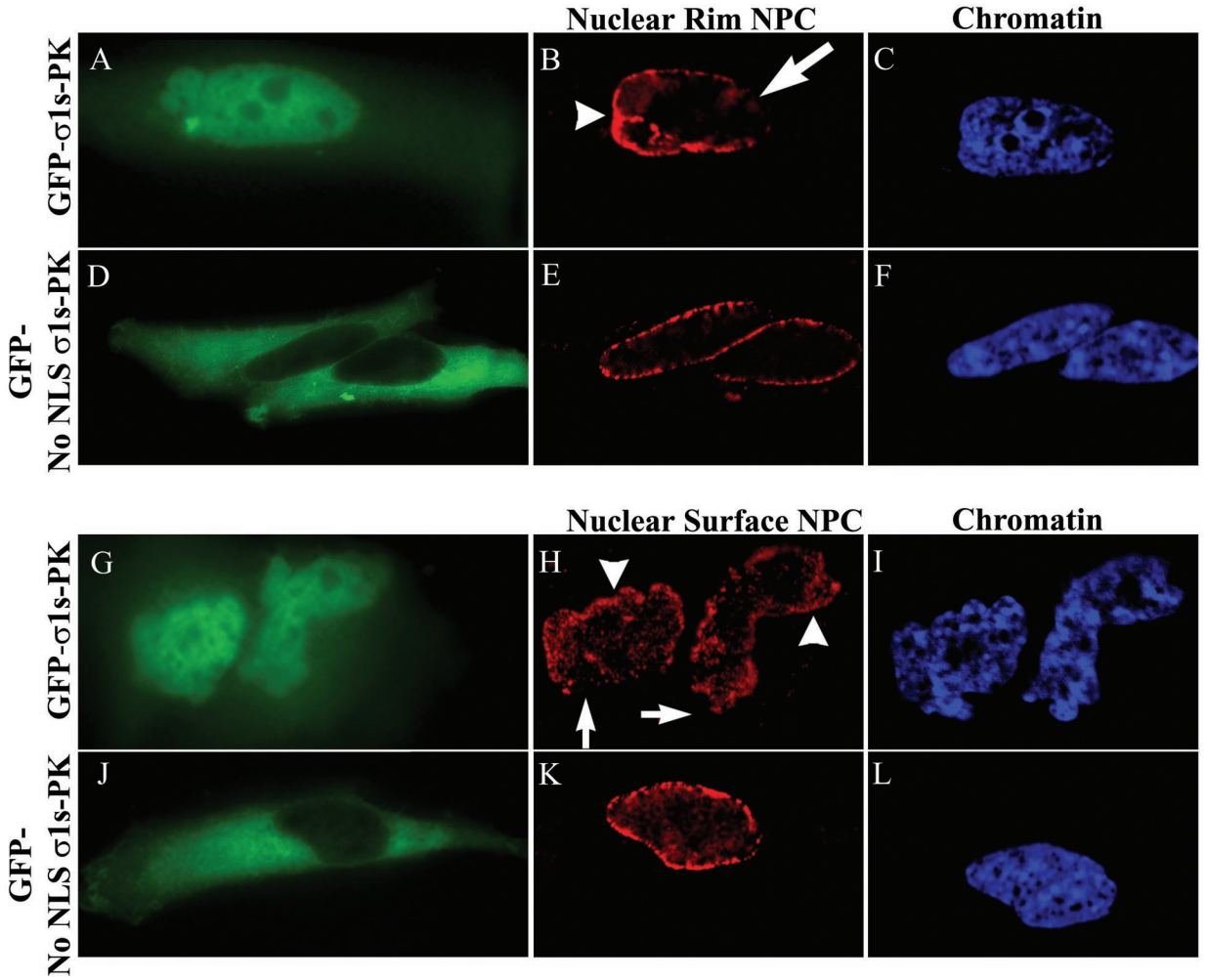


FIG. 6. Nuclear localization of σ1s induces NPC clustering. HeLa cells were transfected with GFP-σ1s-PK (A to C and G to I) or GFP-No NLS σ1s-PK (D to F and J to L). Digital microscopy of NPC nucleoporin-labeled cells expressing GFP-σ1s-PK (A and G) showed clustering of NPCs at the surface of the nucleus (arrowheads in panel H) and at the nuclear rim (arrowheads in panel B), while some areas of the NE were depleted of NPC (arrows in panels B and H). Cells in which σ1s is expressed but is not able to translocate to the nucleus (D and J) showed conventional NPC staining (E and K). Hoechst 33342 dsDNA stain was used to define nuclei (C, F, I, and L).

A-type lamina network and NPCs are perturbed by the translocation of σ1s into the host cell nucleus.

## DISCUSSION

Cytoplasmic reovirus infection profoundly affects the host cell nucleus and its functions (9, 30–32, 41). Recently, we have shown that σ1s plays a key role in determining host cell nuclear function by its capacity to modulate virus-induced $G_2$/M cell cycle arrest in infected cells (31, 32). We now show that the σ1s protein localizes to the nucleus in both infected and transfected cells. Nuclear import of σ1s occurs by an active, NLS-mediated mechanism involving a novel σ1s NLS, $^{15}$RSRRRLK$^{21}$, that is both necessary and sufficient for σ1s nuclear localization.

Upon entering the nucleus, σ1s induces disruptions in chromatin organization, NPC distribution, and nuclear lamina organization, which result in profound distortion of nuclear morphology and in the appearance of a novel type of nuclear herniation containing both σ1s and cellular DNA (Fig. 6A and G and 7A). Both NPCs and the A-type lamina network lose their normal homogenous distribution and become irregularly clustered in specific areas of the NE and subsequently absent from others. It is unclear which of these two disturbances is primary. Although the primary means of herniation development has yet to be determined, σ1s-induced nuclear herniations represent a novel type of virus-induced perturbation of nuclear structure.

Perturbation of the nuclear lamina can grossly alter nuclear shape, induce nuclear herniations and NPC clustering, and alter chromatin organization (10, 13, 21, 23, 36, 42). Vigouroux et al. reported that skin fibroblasts from patients bearing mutations in LaA/C possess nuclei with prominent NE herniations deficient in NPCs and exhibit aberrant chromatin staining (42). Loss of lamin expression in *Caenorhabditis elegans* or *Drosophila* mutants results in spatial disorganization of NPCs, nuclear herniations, chromatin disorganization, and cell cycle inhibi-

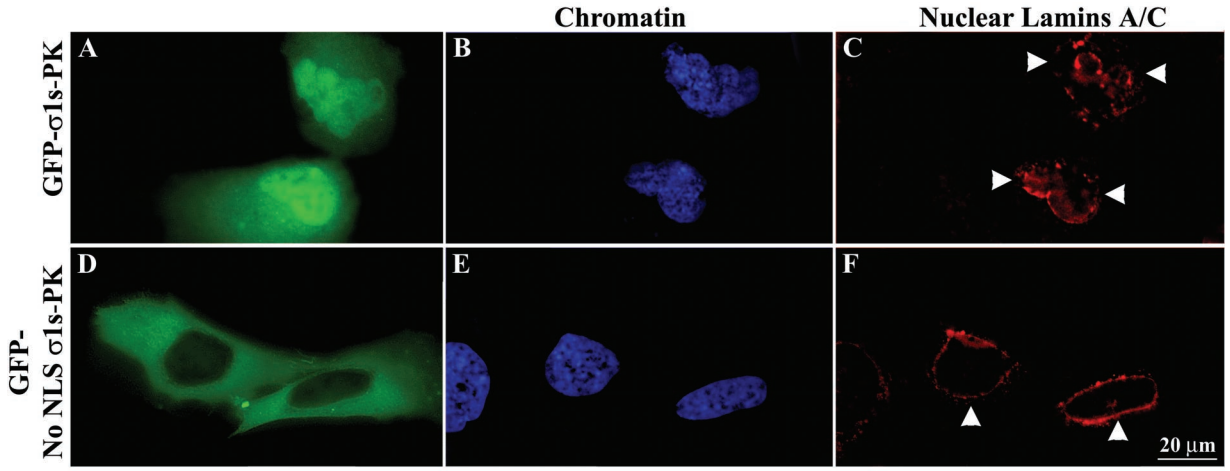


FIG. 7. Nuclear localization of σ1s induces disorganization of the A-type nuclear lamina network. HeLa cells were transfected with GFP-σ1s-PK (A to C) or GFP-No NLS σ1s-PK (D to F). Digital microscopy of LaA/C-labeled cells expressing GFP-σ1s-PK showed delamination of the A-type nuclear lamina network (arrowheads in panel C). Cells in which σ1s is expressed but is not able to translocate to the nucleus showed conventional LaA/C staining (F). Hoechst 33342 dsDNA stain was used to define nuclei (B and E).

tion (21, 23). Like these lamin-based nuclear herniations, σ1s-induced nuclear herniations display similar patterns of lamina disorganization, chromatin staining, and NE shape abnormalities. However, NPC clustering is a prominent feature of σ1s-induced herniations, and although NPC clustering is a result of lamin-based nuclear architecture abnormalities in the *C. elegans* and *Drosophila* systems (21, 23), this has not yet been described for mammalian cells.

An alternative explanation for our findings is that altered NPC structure and distribution may trigger disorganization of the nuclear lamina and its attached chromatin, resulting in the development of nucleoporin-based nuclear herniations. NPCs form an immobile network within the NE and are tethered by the nuclear lamina (8, 21, 23, 39). Wente and Blobel suggested a model in which perturbation of the N terminus of nucleoporin 145p (nup145p) resulted in an irregular NPC distribution, NPC clustering, and multilobulated nuclei with irregular chromatin organization (43). They suggested that loss of the N terminus of nup145p left the NPC unanchored and allowed it to diffuse into the NE, resulting in NPC clustering and nuclear shape abnormalities (43). In yeast two-hybrid experiments, we found that σ1s interacted with mammalian nucleoporin p54 (nup54) (unpublished observation). This suggests the possibility that σ1s may interact with nup54 and destabilize the NPC structure within the NE, allowing the unanchored NPC to migrate and cluster with other destabilized NPCs within the NE. One consequence of the abnormal migration of NPCs is that the attached lamina could become strained and disorganized, in turn altering nuclear morphology and chromatin organization. This model is supported by our data, which show that, similar to the case for nup145pΔN herniations, σ1s expression induces misshapen lobulated nuclei with prominent nuclear herniations, clustered NPCs, and aberrant chromatin staining.

Regardless of whether σ1s-induced nuclear herniations arise from a primary lamina disorganization event or from a primary disturbance in NPC structure, it is interesting to speculate about their potential biological significance. Reovirus infection leads to a $G_2$/M cell cycle arrest in infected cells and is associated with alteration of the activity and phosphorylation status of key $G_2$/M regulatory proteins (31). The phosphorylation state and consequent enzymatic activity of many $G_2$/M proteins are in part dependent upon their subcellular compartmentalization (29). Interestingly, even though reoviruses (which undergo cytoplasmic viral replication) and retroviruses (which undergo nuclear viral replication) differ dramatically in their replicative strategies and structural organizations, the human immunodeficiency virus type 1 Vpr protein has many functional parallels with reovirus σ1s, including the capacity to induce both $G_2$/M cell cycle arrest and nuclear herniations in infected and transfected cells (10, 31–33). It has recently been suggested that Vpr-induced nuclear herniations may serve to dysregulate the compartmentalization of $G_2$/M cell cycle proteins (10). Perhaps σ1s plays an analogous role in reovirus-infected cells. Both Vpr (10)- and σ1s-induced nuclear herniations are characterized by the disorganization of the nuclear lamina and chromatin architecture, yet σ1s-induced nuclear herniations consistently display clustering of NPCs at or near herniation sites, establishing them as a unique type of virus-induced nuclear alteration. It is possible that this disorganization itself plays a role in disrupting cell cycle regulation. *C. elegans* lamin mutants have both abnormal nuclear morphology and the inability to complete the cell cycle (23), and *Xenopus* extracts with disrupted nuclear lamin organization undergo DNA synthesis arrest, in turn prohibiting mitotic progression (25). Taken together, these findings suggest that σ1s may alter nuclear architecture to affect $G_2$/M arrest by either herniating the nucleus or disrupting nuclear lamina organization.

Mechanisms of virus-induced cytopathic effects in infected host cells are complex and only partially defined. Our work presented here identifies a new type of virus-mediated alteration of nuclear architecture and a novel form of virus-induced cytopathic effect. Virus-induced nuclear herniations may well influence regulation of cellular behavior and gene expression

from the nucleus and ultimately disease pathogenesis in the infected host.

## ACKNOWLEDGMENTS

We thank Gary W. Mierau for electron microscopy collaboration. We also thank Warner C. Greene for the generous gift of the pEGFP-PK vector, which was invaluable in our studies, and Terry Dermody for the 2F4 hybridoma cell line.

This work was supported by Public Health Service grant 1RO1AG14071 from the National Institutes of Health (to K.L.T.), Merit and REAP grants from the Department of Veterans Affairs (to K.L.T.), U.S. Army Medical Research and Material Command grant DAMD17-98-1-8614 (to K.L.T.), and the Reuler-Lewin Family Professorship of Neurology (to K.L.T.).

## REFERENCES

1. **Belli, B. A., and C. E. Samuel.** 1991. Biosynthesis of reovirus-specified polypeptides: expression of reovirus S1-encoded sigma 1NS protein in transfected and infected cells as measured with serotype specific polyclonal antibody. Virology **185:**698–709.
2. **Bodoor, K., S. Shaikh, P. Enarson, S. Chowdhury, D. Salina, W. H. Raharjo, and B. Burke.** 1999. Function and assembly of nuclear pore complex proteins. Biochem. Cell Biol. **77:**321–329.
3. **Bogerd, A. M., J. A. Hoffman, D. C. Amberg, G. R. Fink, and L. I. Davis.** 1994. nup1 mutants exhibit pleiotropic defects in nuclear pore complex function. J. Cell Biol. **127:**319–332.
4. **Clarke, P., S. M. Meintzer, L. Moffitt, and K. L. Tyler.** 2003. Two distinct phases of virus-induced NF-kappaB-regulation enhance TRAIL-mediated apoptosis in virus-infected cells. J. Biol. Chem. **278:**18092–18100.
5. **Clarke, P., S. M. Meintzer, C. Widmann, G. L. Johnson, and K. L. Tyler.** 2001. Reovirus infection activates JNK and the JNK-dependent transcription factor c-Jun. J. Virol. **75:**11275–11283.
6. **Connolly, J. L., S. E. Rodgers, P. Clarke, D. W. Ballard, L. D. Kerr, K. L. Tyler, and T. S. Dermody.** 2000. Reovirus-induced apoptosis requires activation of transcription factor NF-κB. J. Virol. **74:**2981–2989.
7. **Conti, E.** 2002. Structures of importins, p. 93–113. *In* K. Weis (ed.), Nuclear transport. Springer-Verlag, Heidelberg, Germany.
8. **Daigle, N., J. Beaudouin, L. Hartnell, G. Imreh, E. Hallberg, J. Lippincott-Schwartz, and J. Ellenberg.** 2001. Nuclear pore complexes form immobile networks and have a very low turnover in live mammalian cells. J. Cell Biol. **154:**71–84.
9. **DeBiasi, R. L., P. Clarke, S. Meintzer, R. Jotte, B. K. Kleinschmidt-Demasters, G. L. Johnson, and K. L. Tyler.** 2003. Reovirus-induced alteration in expression of apoptosis and DNA repair genes with potential roles in viral pathogenesis. J. Virol. **77:**8934–8947.
10. **de Noronha, C. M., M. P. Sherman, H. W. Lin, M. V. Cavrois, R. D. Moir, R. D. Goldman, and W. C. Greene.** 2001. Dynamic disruptions in nuclear envelope architecture and integrity induced by HIV-1 Vpr. Science **94:**1105–1108.
11. **Dermody, T. S., M. L. Nibert, R. Bassel-Duby, and B. N. Fields.** 1990. Sequence diversity in S1 genes and S1 translation products of 11 serotype 3 reovirus strains. J. Virol. **64:**4842–4850.
12. **Enninga, J., D. E. Levy, G. Blobel, and B. M. Fontoura.** 2002. Role of nucleoporin induction in releasing an mRNA nuclear export block. Science **295:**1523–1525.
13. **Favreau, C., E. Dubosclard, C. Ostlund, C. Vigouroux, J. Capeau, M. Wehnert, D. Higuet, H. J. Worman, J. C. Courvalin, and B. Buendia.** 2003. Expression of lamin A mutated in the carboxyl-terminal tail generates an aberrant nuclear phenotype similar to that observed in cells from patients with Dunnigan-type partial lipodystrophy and Emery-Dreifuss muscular dystrophy. Exp. Cell Res. **282:**14–23.
14. **Fortes, P., A. Beloso, and J. Ortin.** 1994. Influenza virus NS1 protein inhibits pre-mRNA splicing and blocks mRNA nucleocytoplasmic transport. EMBO J. **13:**704–712.
15. **Fouchier, R. A., B. E. Meyer, J. H. Simon, U. Fischer, A. V. Albright, F. Gonzalez-Scarano, and M. H. Malim.** 1998. Interaction of the human immunodeficiency virus type 1 Vpr protein with the nuclear pore complex. J. Virol. **72:**6004–6013.
16. **Glass, J. R., and L. Gerace.** 1990. Lamins A and C bind and assemble at the surface of mitotic chromosomes. J. Cell Biol. **111:**1047–1057.
17. **Gustin, K. E., and P. Sarnow.** 2001. Effects of poliovirus infection on nucleocytoplasmic trafficking and nuclear pore complex composition. EMBO J. **20:**240–249.
18. **Gustin, K. E., and P. Sarnow.** 2002. Inhibition of nuclear import and alteration of nuclear pore complex composition by rhinovirus. J. Virol. **76:**8787–8796.
19. **Hirano, M., S. Kaneko, T. Yamashita, H. Luo, W. Qin, Y. Shirota, T. Nomura, K. Kobayashi, and S. Murakami.** 2003. Direct interaction between nucleolin and hepatitis C virus NS5B. J. Biol. Chem. **278:**5109–5115.
20. **Hutchison, C. J.** 2002. Lamins: building blocks or regulators of gene expression? Nat. Rev. Mol. Cell Biol. **3:**848–858.
21. **Lenz-Bohme, B., J. Wismar, S. Fuchs, R. Reifegerste, E. Buchner, H. Betz, and B. Schmitt.** 1997. Insertional mutation of the Drosophila nuclear lamin Dm0 gene results in defective nuclear envelopes, clustering of nuclear pore complexes, and accumulation of annulate lamellae. J. Cell Biol. **137:**1001–1016.
22. **Lim, C., D. Lee, T. Seo, C. Choi, and J. Choe.** 2003. Latency-associated nuclear antigen of Kaposi's sarcoma-associated herpesvirus functionally interacts with heterochromatin protein 1. J. Biol. Chem. **278:**7397–7405.
23. **Liu, J., T. R. Ben Shahar, D. Riemer, M. Treinin, P. Spann, K. Weber, A. Fire, and Y. Gruenbaum.** 2000. Essential roles for *Caenorhabditis elegans* lamin gene in nuclear organization, cell cycle progression, and spatial organization of nuclear pore complexes. Mol. Biol. Cell. **11:**3937–3947.
24. **Moir, R. D., and T. P. Spann.** 2001. The structure and function of nuclear lamins: implications for disease. Cell Mol. Life Sci. **58:**1748–1757.
25. **Moir, R. D., T. P. Spann, H. Herrmann, and R. D. Goldman.** 2000. Disruption of nuclear lamin organization blocks the elongation phase of DNA replication. J. Cell Biol. **149:**1179–1192.
26. **Muranyi, W., J. Haas, M. Wagner, G. Krohne, and U. H. Koszinowski.** 2002. Cytomegalovirus recruitment of cellular kinases to dissolve the nuclear lamina. Science **297:**854–857.
27. **Petersen, J. M., L. S. Her, and J. E. Dahlberg.** 2001. Multiple vesiculoviral matrix proteins inhibit both nuclear export and import. Proc. Natl. Acad. Sci. USA **98:**8590–8595.
28. **Petersen, J. M., L. S. Her, V. Varvel, E. Lund, and J. E. Dahlberg.** 2000. The matrix protein of vesicular stomatitis virus inhibits nucleocytoplasmic transport when it is in the nucleus and associated with nuclear pore complexes. Mol. Cell. Biol. **20:**8590–8601.
29. **Pines, J.** 1999. Four-dimensional control of the cell cycle. Nat. Cell Biol. **1:**E73–E79.
30. **Poggioli, G. J., R. L. DeBiasi, R. Bickel, R. Jotte, A. Spalding, G. L. Johnson, and K. L. Tyler.** 2002. Reovirus-induced alterations in gene expression related to cell cycle regulation. J. Virol. **76:**2585–2594.
31. **Poggioli, G. J., T. S. Dermody, and K. L. Tyler.** 2001. Reovirus-induced σ1s-dependent $G(_2)$/M phase cell cycle arrest is associated with inhibition of p34 (cdc2). J. Virol. **75:**7429–7434.
32. **Poggioli, G. J., C. Keefer, J. L. Connolly, T. S. Dermody, and K. L. Tyler.** 2000. Reovirus-induced $G(_2)$/M cell cycle arrest requires σ1s and occurs in the absence of apoptosis. J. Virol. **74:**9562–9570.
33. **Poon, B., K. Grovit-Ferbas, S. A. Stewart, and I. S. Chen.** 1998. Cell cycle arrest by Vpr in HIV-1 virions and insensitivity to antiretroviral agents. Science **281:**266–269.
34. **Rodgers, S. E., J. L. Connolly, J. D. Chappell, and T. S. Dermody.** 1998. Reovirus growth in cell culture does not require the full complement of viral proteins: identification of a σ1s-null mutant. J. Virol. **72:**8597–8604.
35. **Rohr, O., D. Lecestre, S. Chasserot-Golaz, C. Marban, D. Avram, D. Aunis, M. Leid, and E. Schaeffer.** 2003. Recruitment of Tat to heterochromatin protein HP1 via interaction with CTIP2 inhibits human immunodeficiency virus type 1 replication in microglial cells. J. Virol. **77:**5415–5427.
36. **Schirmer, E. C., T. Guan, and L. Gerace.** 2001. Involvement of the lamin rod domain in heterotypic lamin interactions important for nuclear organization. J. Cell Biol. **153:**479–489.
37. **Scott, E. S., and P. O'Hare.** 2001. Fate of the inner nuclear membrane protein lamin B receptor and nuclear lamins in herpes simplex virus type 1 infection. J. Virol. **75:**8818–8830.
38. **Sherman, M. P., C. M. de Noronha, M. I. Heusch, S. Greene, and W. C. Greene.** 2001. Nucleocytoplasmic shuttling by human immunodeficiency virus type 1 Vpr. J. Virol. **75:**1522–1532.
39. **Stuurman, N., S. Heins, and U. Aebi.** 1998. Nuclear lamins: their structure, assembly, and interactions. J. Struct. Biol. **122:**42–66.
40. **Tyler, K. L., P. Clarke, R. L. DeBiasi, D. Kominsky, and G. J. Poggioli.** 2001. Reoviruses and the host cell. Trends Microbiol. **9:**560–564.
41. **Tyler, K. L., M. K. Squier, S. E. Rodgers, B. E. Schneider, S. M. Oberhaus, T. A. Grdina, J. J. Cohen, and T. S. Dermody.** 1995. Differences in the capacity of reovirus strains to induce apoptosis are determined by the viral attachment protein sigma 1. J. Virol. **69:**6972–6979.
42. **Vigouroux, C., M. Auclair, E. Dubosclard, M. Pouchelet, J. Capeau, J. C. Courvalin, and B. Buendia.** 2001. Nuclear envelope disorganization in fibroblasts from lipodystrophic patients with heterozygous R482Q/W mutations in the lamin A/C gene. J. Cell Sci. **114:**4459–4468.
43. **Wente, S. R., and G. Blobel.** 1994. NUP145 encodes a novel yeast glycine-leucine-phenylalanine-glycine (GLFG) nucleoporin required for nuclear envelope structure. J. Cell Biol. **125:**955–969.
44. **Wurm, T., H. Chen, T. Hodgson, P. Britton, G. Brooks, and J. A. Hiscox.** 2001. Localization to the nucleolus is a common feature of coronavirus nucleoproteins, and the protein may disrupt host cell division. J. Virol. **75:**9345–9356.
45. **Zolotukhin, A. S., and B. K. Felber.** 1999. Nucleoporins nup98 and nup214 participate in nuclear export of human immunodeficiency virus type 1 Rev. J. Virol. **73:**120–127.